Mutation of the IFNAR-1 Receptor Binding Site of Human IFN-α2 Generates Type I IFN Competitive Antagonists[†]

Manjing Pan,[‡] Eyal Kalie,[§] Brian J. Scaglione,[||] Elizabeth S. Raveche,[||] Gideon Schreiber,[§] and Jerome A. Langer*[,‡]

Department of Molecular Genetics, Microbiology, and Immunology, UMDNJ—Robert Wood Johnson Medical School, Piscataway, New Jersey 08854, Department of Pathology and Laboratory Medicine, UMDNJ—New Jersey Medical School, Newark, New Jersey 07103, and Department of Biological Chemistry, Weizmann Institute of Science, Rehovot IL-76100, Israel

Received August 22, 2008; Revised Manuscript Received September 17, 2008

ABSTRACT: Type I interferons (IFNs) are multifunctional cytokines that activate cellular responses by binding a common receptor consisting of two subunits, IFNAR-1 and IFNAR-2. Although the binding of IFNs to IFNAR-2 is well characterized, the binding to the lower affinity IFNAR-1 remains less well understood. Previous reports identified a region of human IFN-α2 on the B and C helices ("site 1A": N65, L80, Y85, Y89) that plays a key role in binding IFNAR-1 and contributes strongly to differential activation by various type I IFNs. The current studies demonstrate that residues on the D helix are also involved in IFNAR-1 binding. In particular, residue 120 (Arg in IFN-α2; Lys in IFN-α2/α1) appears to be a "hot-spot" residue: substitution by alanine significantly decreased biological activity, and the charge-reversal mutation of residue 120 to Glu caused drastic loss of antiviral and antiproliferative activity for both IFN-α2 and IFN-α2/α1. Mutations in residues of helix D maintained their affinity for IFNAR-2 but had decreased affinity for IFNAR-1. Single-site or multiple-site mutants in the IFNAR-1 binding site that had little or no detectable *in vitro* biological activity were capable of blocking *in vitro* antiviral and antiproliferative activity of native IFN-α2; i.e., they are type I IFN antagonists. These prototype IFN antagonists can be developed further for possible therapeutic use in systemic lupus erythematosus, and analogous molecules can be designed for use in animal models.

Type I interferons are a family of cytokines characterized by their antiviral, antiproliferative, and immunomodulatory activities (*4*). For mammals, the type I interferons include the IFN-α and IFN-β subtypes and may include other subtypes, such as IFN-ω, IFN-κ, IFN-ϵ, IFN-δ, and IFN-τ. Humans express 13 IFN-αs and 1 each of IFN-β, IFN-ω, IFN-ϵ, and IFN-κ. The structures of the type I IFNs[1] are homologous (reviewed in ref *5*), consisting of a five-helix bundle (labeled sequentially "A" to "E") with a functionally important long loop ("AB loop") connecting helices A and B. In spite of the high homology and sequence conservation of different IFN subtypes, individual subtypes display different profiles of biological activities, including antiproliferative, antiviral, and immunomodulatory.

IFNs are used clinically for the treatment of various pathologies, including virus infections, tumors, and multiple sclerosis. However, there is strong evidence that type I interferons are inappropropriately expressed in individuals with systemic lupus erythematosus (SLE) and are involved in lupus development and/or progression (reviewed, for instance, in refs *6* and *7*). IFN antagonists are therefore needed for possible therapeutic application in SLE and for studies in model systems, such as murine strains that develop lupus-like disease.

Type I IFNs activate cellular responses by binding a common high-affinity cell surface receptor consisting of two transmembrane protein subunits, IFNAR-1 and IFNAR-2, which make distinct contributions to ligand binding (*8, 9*; reviewed in ref *10*). Binding of interferon to its receptor complex initiates activation of the Jak/STAT pathway and other signal transduction pathways, leading to the regulation of relevant genes.

The subunits of IFNAR make distinct contributions to ligand binding. Human and mouse IFNAR-1 have low but varied intrinsic affinity for the various IFNs (K_D ~0.05−5 μM), whereas IFNAR-2 has moderate to high affinity for IFNs (K_D 0.1−100 nM) (*8, 9, 11, 12*). Receptor binding appears to be a sequential process, with IFN first binding to the higher affinity IFNAR-2, followed by recruitment of IFNAR-1, to form the ternary complex, with consequent

[†] Supported by a research award from the Alliance for Lupus Research to J.A.L. and by funding from the Foundation of UMDNJ. This work was also supported by the Israel Science Foundation funded by the Israel Academy of Sciences and Humanities to G.S. (grant 633/06).

* To whom correspondence should be addressed. E-mail: langer@umdnj.edu. Phone: 732-235-5224. Fax: 732-235-5223.

[‡] UMDNJ—Robert Wood Johnson Medical School.

[§] Weizmann Institute of Science.

[||] UMDNJ—New Jersey Medical School.

[1] Abbreviations: CRF-2, cytokine receptor family 2; DMEM, Dulbecco's modified Eagle's medium; EC_{50}, effective concentration for 50% of maximum effect; ECD, extracellular domain; EDC, *N*-(3-dimethylaminopropyl)-*N*′-ethylcarbodiimide; EDTA, ethylenediaminetetraacetic acid; EMCV, encephalomyocarditis virus; FNIII, fibronectin type III domain; GuHCl, guanidine hydrochloride; IB, inclusion body; IFN, interferon; IC_{50}, concentration for 50% inhibition; IL-1, interleukin 1; IL-1R, interleukin 1 receptor; IL-1RA, interleukin 1 receptor antagonist; K_D, equilibrium dissociation constant; NHS, *N*-hydroxysuccinimide; NMR, nuclear magnetic resonance; PMSF, phenylmethanesulfonyl fluoride; SPR, surface plasmon resonance; VSV, vesicular stomatitis virus.

10.1021/bi801588g CCC: $40.75
Published on Web 10/21/2008

receptor and cellular activation (*13*−*15*). However, the details of the interactions, particularly the differences in IFNAR-1 binding, seem key to differential cellular activation (*9, 13*).

IFNAR-2 is the major ligand-binding component of the type I IFN receptor and has an extracellular domain (ECD) consisting of two fibronectin type III (FNIII) domains. IFN binding to IFNAR-2 generally has high (nanomolar) affinity (*9, 16*), and the complementary binding sites on both IFN and IFNAR-2 were well characterized by a combination of mutagenesis and NMR studies of both the IFNAR-2 ECD and the IFN-α2/IFNAR-2 ECD complex (*17*−*19*). On IFN-α2, the key residues for interacting with IFNAR-2 form a contiguous patch contributed by residues from the A helix, AB loop, and E helix (*20*). The C-terminal eight amino acids of type I IFNs, which show considerable variation, can modulate the affinity for IFNAR-2 by 20-fold (*21*).

The binding of type I IFNs to the IFNAR-1 receptor is relatively weak, transient, and less well understood, and our understanding of IFN/IFNAR-1 interactions has been limited by the large size of IFNAR-1 and the lower affinity of the IFN/IFNAR-1 interaction. The extracellular domain of IFNAR-1 consists of four FNIII domains of approximately 100 amino acids each. Mutagenesis studies and interspecies chimeric receptors have provided some information about ligand-binding regions (*8, 11, 12, 22*). Although no high-resolution structural studies of the IFNAR-1 ECD have appeared, a low-resolution structure of the IFN-α2/IFNAR-1-ECD/IFNAR-2-ECD complex was obtained by density-modeling to a three-dimensional image reconstruction of electron microscopy images and suggests a "wrap-around" interaction of IFNAR-1 with IFN (*23, 24*), subsequent to a conformational change (*24*).

Identification of the IFNAR-1 binding site on type I IFNs has emerged more slowly. Various studies implicated residues on helices B, C, and D and the DE loop in IFN activity, with some studies suggesting that these regions might be involved in receptor binding, possibly IFNAR-1 binding (*12, 25*−*28*). Recently, Roisman et al. found that residues N65, L80, Y85, and Y89 on the B and C helices, with N65, Y85, and Y89 forming a contiguous patch (here termed site 1A), are important for IFN-α2 binding to IFNAR-1 (*41*). When mutated individually to alanine, there were small decreases in biological activity consequent to small decreases in the affinity for IFNAR-1. The combined four-site alanine substitution mutant ("NLYY") retained about 1% of its antiviral activity and 0.1% of its antiproliferative activity. The neighboring residues of IFN-α2, H57, E58, and Q61, are also part of the IFNAR-1 binding site. However, mutating any of them to alanine *increases* affinity for IFNAR-1 and *increases* activity, particularly antiproliferative activity. The triple alanine mutation ("HEQ") has significantly higher antiproliferative activity and affinity for IFNAR-1 (*13*). It was further shown that a three-point substitution of HEQ to YNS, obtained by phage-display techniques, greatly enhances IFN affinity for IFNAR-1 and can selectively enhance antiproliferative and antitumor activities (*29*). These experiments gave rise to a model wherein the strength of the IFN/IFNAR-1 interaction is a key determinant for differential cellular activation by type I IFNs (see also refs *10* and *30*).

An IFN-α analogue with competitive antagonist properties can, in principle, be engineered that binds with high affinity to IFNAR-2 but where the low-affinity site for IFNAR-1 has been effectively eliminated. However, the residual activity of the NLYY mutant leaves this as a weak agonist and suggests that other residues are also involved in IFNAR-1 binding. Following previous studies (*25*−*27, 31*−*33*), we have investigated possible contributions of residues on the D helix. These studies have led to the identification of additional residues that contribute to IFNAR-1 binding and have permitted the construction of IFN-α2 analogues with *in vitro* antagonist activity.

MATERIALS AND METHODS

Cell Culture. Human HeLa and WISH cells and bovine MDBK cells were grown in Dulbecco's modified Eagle's medium (DMEM) supplemented with 10% cosmic calf serum (Hyclone) with glutamax (Sigma). Murine L-929 cells were cultured in minimum essential Eagle's medium with glutamax at 37 °C and 5% CO_2. NFS-1.0 cells (ATCC CRL-1705), a murine line that is highly sensitive to the antiproliferative effects of IFN, were cultured in RPMI 1640 supplemented with 15% cosmic calf serum, 5 mM L-glutamine, 1% penicillin−streptomycin (Mediatech, Inc.), 1× HEPES buffer (Mediatech), 0.1% 2-mercaptoethanol (Gibco), 2.5 g/L D-glucose (Gibco), and 1 mM sodium pyruvate (Gibco).

Construction of IFN-α2b and IFN-α2/α1 Variants. The cDNA (cDNA) representing the 165 amino acid coding region of IFN-α2b, followed by a codon representing a translational "stop" signal ("TGA") was supplied by Dr. Sergei Kotenko (UMDNJ—New Jersey Medical School). Human-derived chimeric IFN-α2/α1 ("IFN-αA/D") cDNA was kindly provided by Dr. Sidney Pestka (UMDNJ—Robert Wood Johnson Medical School), and the cDNA fragment was restricted and cloned into *Bam*HI/*Nde*I-digested pET-11a vector (Novagen).

Site-directed mutagenesis (QuickChange kit; Stratagene) was used to create a series of human IFN-α2 and IFN-α2/α1 variants. For improving IFN-α2/α1 and IFN-α2 expression in *Escherichia coli* strain BL21 (DE3) Rosetta 2 (Novagen), the high-frequency arginine codons CGC or CGG were substituted for the native codons, AGA or ACG, at positions 12, 13, and 33 (*34*). All constructs were confirmed by DNA sequencing of both DNA strands with an automated DNA system.

Protein Expression. All plasmid DNAs of IFN-α2 and IFN-α2/α1 mutants were individually transformed into *E. coli* strain BL21 (DE3) Rosetta 2 (Novagen). Bacteria were grown overnight in LB broth containing 100 μg/mL ampicillin at 37 °C. The cultures were then diluted 50-fold and incubated at 37 °C with shaking. Protein expression was induced by addition of isopropyl β-D-thiogalactoside to 0.8 mM. The bacteria were then incubated at the same temperature for 4−6 h.

The cells were harvested by centrifugation and resuspended in buffer A (50 mM Tris-HCl, pH 8.0, 40 mM NaCl, 5 mM EDTA) supplemented with lysozyme (0.2 mg/mL) and 0.2 mM PMSF (phenylmethanesulfonyl fluoride; Sigma). The resuspended cells were sonicated on ice (3 × 15 s pulses at 50 W). Triton X-100 (1%; Bio-Rad) was added to the homogeneous suspension after sonication, incubated overnight at 30 °C, and then centrifuged for 20 min at 30000*g*.

The pellet [inclusion body (IB)] was either solubilized immediately or stored frozen at −80 °C until further use.

The IB pellet was solubilized in 7 M GuHCl (guanidine hydrochloride; Invitrogen) in buffer A overnight at 4 °C with gentle shaking. The IB solution was then centrifuged at 30000*g* for 30 min at 4 °C. The supernatant was refolded by dropwise dilution into 15 volumes of 0.5 M L-arginine (Sigma) in buffer A for 24−48 h at 4 °C (*35*). The refolded solution was adjusted to 1.6 M $(NH_4)_2SO_4$ (Sigma, Ultrapure) for protein purification.

The refolded protein supernatant was loaded on a hydrophobic column (Toyopearl Phenyl-650M; Tosoh Biosciences) preequilibrated with 0.5 M GuHCl, 50 mM Tris-HCl, pH 8.0, and 1.6 M $(NH_4)_2SO_4$. The column was washed with the buffer containing 0.5 M GuHCl, 50 mM Tris-HCl, pH 8.0, 1.6 M $(NH_4)_2SO_4$, and 1 M urea (Sigma, Ultrapure). The proteins were eluted with the buffer containing 0.5 M GuHCl, 50 mM Tris-HCl, pH 8.0, and 1 M urea.

The fractions with IFN were dialyzed against 20 volumes of 20 mM Tris-HCl, pH 8.0, and 50 mM NaCl overnight at 4 °C. The dialyzed supernatant was applied to a HiTrap Fast-Flow Q-Sepharose ion-exchange column (Amersham Bioscience) and eluted with a linear gradient of 50−500 mM NaCl. Samples were further concentrated, and buffer was exchanged to the storage buffer of 20 mM Tris-HCl, pH 8.0, 50 mM NaCl, and 6% glycerol. Purity of proteins was determined by SDS−polyacrylamide gel electrophoresis, and the concentration was determined by absorbance at 280 nm with a calculated molar extinction coefficient: $E = 18950$ (IFN-α2); $E = 17585$ (IFN-α2/α1).

In later experiments, proteins were further purified on a Superose 12 HR 10/30 column with the ÄKTA-FPLC system (Amersham Pharmacia Biotech). The column was developed in the buffer containing 50 mM Tris-HCl, pH 8.4, 100 mM NaCl, and 6% glycerol at a constant flow rate of 0.5 mL/min.

Antiviral and Antiproliferative Assays. Antiviral activity of wild-type and mutant IFNs was assayed as the inhibition of the cytopathic effect of vesicular stomatitis virus (VSV) on human HeLa, WISH, or A-549 cells and bovine MDBK cells and with encephalomyocarditis virus (EMCV) on murine L-929 cells (*36*). Assays on bovine MDBK cells were included because bovine cells respond with high-level activity to all native human IFN-αs, and some modifications of human IFN-α structure that cause dramatic changes in activity on human cells have minimal effects on the activity measured on MDBK cells. This is likely due to the high affinity of human IFN-αs for bovine IFNAR-1 (*2, 37*).

For antiproliferative assays with WISH and L-929 cells, cells (usually $\sim 1 \times 10^4$) in 50 μL of growth medium were added to serial dilutions of IFNs in a 96-well culture dish. Cells were grown for 3−4 days. Medium was removed, and cells were stained with crystal violet. Plates were read by eye to find the dilution corresponding to 50% of maximum growth. Alternatively, the crystal violet in the stained cells was solubilized by addition of 100 μL of 50% ethanol/50% Tris-HCl (pH 8.0) (v/v). Optical density was read at 586 nm. For WISH cells, the cells released from the plates and may have undergone cell death during the assay. Data were analyzed by a nonlinear fit to a sigmoidal curve, and the EC_{50} and statistical parameters were calculated from the curve using the program "Prism v. 3" (GraphPad, Inc., San Diego, CA).

For antiproliferative assays with NFS-1.0 cells, cells (5×10^3; 100 μL) with an initial viability of >90% were added to 96-well plates containing 40 μL of serial dilutions of native or mutant IFNs. After 72 h of incubation, cell density was determined with the Celltiter 96 nonradiactive cell proliferation assay (Promega). Briefly, 20 μL of dye solution per 100 μL of culture medium was added to each well and incubated at 37 °C for 3−4 h. Then 100 μL of solubilization solution/stop mix was added to each well. After 1 h at 37 °C or up to 72 h at room temp, the contents of the wells were mixed for uniformity, and the plate was read at 570 nm with a standard 96-well plate reader. Murine NFS-01 cells showed up to an 80% reduction in growth from untreated cells. Data were analyzed by a nonlinear fit to a sigmoidal curve, and the EC_{50} and statistical parameters were calculated from the curve using the program "Prism v. 3" (GraphPad, Inc., San Diego, CA).

Antagonism Assays. Antagonism assays were variations of the antiviral cytopathic effect assay and antiproliferative assays (*3, 36*). For the antiviral assay, a constant amount of IFN-α2 (usually $(1-2) \times 10^{-10}$ M, final concentration, depending on the cell type) was combined with serial dilutions of each IFN variant (the highest concentration of each mutant was in the range of $(1-5) \times 10^{-6}$ M, depending on its ability to inhibit IFN activity). Cells were added and incubated overnight at 37 °C and 5% CO_2. VSV was added, and the plates were incubated for 24−30 h. When the cytopathic effect in control wells reached 100%, the plates were stained by crystal violet. In these assays, the active and inactive IFNs could be premixed at room temperature, followed by addition of cells and incubation at 37 °C; i.e., antagonism did not require preincubation of cells with the mutant IFN prior to addition of active IFN-α2. Antiproliferative assays were similarly designed, where a constant amount of IFN-α2, sufficient for growth inhibition of each cell line, was added to serially diluted (usually 2-fold) concentrations of each IFN variant. Cells were added and grown for 3 days. Cells were stained with crystal violet.

Measurement of Binding Affinity. Binding to purified human IFNAR-1 and IFNAR-2 is measured with the protein interaction array system (Bio-Rad) according to published methods (*21*). A solution of 0.005% Tween 20 in PBS, pH 7.4, was used as running buffer at a flow rate of 30 μL/min. For immobilization, an activated EDC/NHS surface was covered with the nonneutralizing antibodies DB2 (*38*) and 46.10 (*39*) against IFNAR1-ECD and IFNAR2-ECD, respectively, and blocked with ethanolamine. Thereafter, five of the six channels were reacted with IFNAR1-ECD or IFNAR2-ECD (180 μL at a concentration of 0.5 μM), leaving one channel free as reference. This was followed by cross-linking a second antibody, AA3 for IFNAR1-ECD and 117.7 for IFNAR2-ECD, to improve the stability of coupling and reduce leakage of IFNAR2-ECD without affecting ligand binding (*40*). Interferons were then injected perpendicular to ligands, at six different concentrations within a range of 37−8000 nM for IFNAR1 binding and 3.12−100 nM for IFNAR2 binding. Data were analyzed with the BIAeval 4.1 software, using the standard Langmuir models for fitting kinetic data. Dissociation constants K_D were determined from the rate constants according to

$$K_D = \frac{k_{off}}{k_{on}} \quad (1)$$

or from the equilibrium response at six different analyte concentration, fitted to the mass-action equation (*21*).

RESULTS

Helix D Residues Are Important for IFN-α2 Activity and Binding to IFNAR-1. Previous examination of the B and C helices of IFN-α2 identified a number of residues that contribute to IFNAR-1 binding (*41*). Single-site alanine substitution mutations, however, did not have dramatic effects, and even the four-site NLYY mutant (NLYY = N65A/L80A/Y85A/Y89A) of the IFNAR-1 binding region retained about 1% antiviral activity and 0.1% antiproliferative activity. Since other studies had implicated parts of helix D in IFN activity and possibly in receptor binding (*25*−*27, 31*−*33*), we examined the D helix of IFN-α2 for residues that might also contribute to IFNAR-1 binding. The D helix contains several strongly conserved features including a positively charged patch (in IFN-α2, R120, K121, Q124, and R125; although Q124 in IFN-α2 was not examined in this study, we did examine the equivalent R124 of IFN-α2/α1; see below), the conserved Leu 117, and Asp 114 (Figure 1). This helix is relatively far from the identified IFNAR-2 binding site.

Within the conserved positively charged residues of helix D, substitution of R120 with alanine decreased antiviral activity to 1−3% and reduced antiproliferative activity to about 0.05% of native IFN-α2 (Figure 2, Table 1). More dramatic loss of activity occurred with the charge-reversal R120E mutation, where activity was below the threshold of the measurements. Furthermore, when the IFN-α2[R120E] mutation is combined with the carboxyl-terminal eight amino acids found in IFN-α8 ("120E-8CTail"), which is reported to increase the affinity for IFNAR-2 (*21*), the antiviral activity on HeLa cells was still not detected. The two-site R120A/K121A mutant had similar activity to R120A, suggesting a less important role for K121A, which was not evaluated as a single-site mutant. The R120E/K121E mutant, similar to the single R120E mutant, had no demonstrable antiviral or antiproliferative activity on human cells and showed a modest (10-fold) decrease of antiviral activity on bovine cells. Moving further along the helix, the charge-reversal R125E mutant had little or no effect on biological activity. Thus, for IFN-α2, substitutions in the positively charged cluster show their relative important in the order R120 ≫ K121 > R125. Leucine 117 is completely conserved in human and murine type I IFNs, is surface-exposed, and is adjacent to R120. Its substitution by alanine decreased antiviral and antiproliferative activity about 5-fold. In combination with R120A, L117A further decreases the antiviral and antiproliferative activity. At the N-terminus of helix D is Asp114, conserved in human and murine IFN-αs but variable in the other type I IFNs. Its substitution by alanine has no effect on antiviral and antiproliferative activity, measured on WISH cells, and a small effect on antiviral activity measured on HeLa cells. Most single-site mutants retained activity on

```
                          HELIX B                          HELIX C
Hu-α2       49-KAETIPVLHEMIQQIFNLFSTKDSS  78-ETLLDKFYTELYQQLNDLEACV
Hu-α1          KAPAISVLHELIQQIFNLFTTKDSS     EDLLDKFCTELYQQLNDLEACV
Hu-α2/α1       KAETIPVLHEMIQQIFNLFTTKDSS     EDLLDKFCTELYQQLNDLEACV
Mu-α4          KAQAILVLRDLTQQILNLFTSKDLS     ATLLDSFCNDLHQQLNDLKACV
Mu-α12         KAQVIPVLSELTQQILTLFTSKDSS     TTLLDSFCNDLHQQLNDLQGCL
Hu-ω           KAHVMSVLHEMLQQIFSLFHTERSS     MTLLDQLHTGLHQQLQHLETCL
Hu-β           KEDAAVTIYEMLQNIFAIFRQDSSS     ETIVENLLANVYHQRNHLKTVLEEKL
Hu-κ           KRDIKKAFYEMSLQAFNIFSQH-TF     ERHLKQIQIGLDQQAEYLNQCL
Hu-ε           KGHTLAILHEMLQQIFSLFRANISL     ENHTEKFLIQLHQQLEYLEALM
Mu-β           KSYTAFAIQEMLQNVFLVFRNNFSS     ETIVVRLLDELHQQTVFLKTVL
Mu-limitin     LGETTSCYSQTLRQVLHLFDTEASR     ERALDQLLSSLWRELQVLKRPR

                          HELIX D
Hu-α2      112-KEDSILAVRKYFQRITLYLKEKK
Hu-α1         -NADSILAVKKYFRRITLYLTEKK
Hu-α2/α1      -KEDSILAVKKYFRRITLYLTEKK
Mu-α4         -QEDSLLAVRTYFHRITVYLRKKK
Mu-α12        -QEDSLLAVRKYFHRITVYLREKK
Hu-ω          -ISSPALTLRRYFQGIRVYLKEKK
Hu-β          -KRMSSLHLKRYYGRILHYLKAKE
Hu-κ          -PQLSSLELRRYFHRIDNFLKEKK
Hu-ε          -SDNLRLQVKMYFRRIHDYLENQD
Mu-β          -MSSTALHLKSYYWRVQRYLKLMK
Mu-limitin    -PLPFALAIRTYFRGFFRYLKAKA
```

FIGURE 1: Alignment of human and murine type I interferon sequences for helices B, C, and D. Experimentally determined α helices are indicated in italics and underlined (PDB entries: HuIFN-α2, 1ITF; HuIFN-*β*, 1AU1; MuIFN-*β*, 1IFA). Sequence numbers for the first residue of each segment are indicated for IFN-α2 and are the same for IFN-α2/α1. Other human IFN-αs contain one additional amino acid, generally indicated as residue 44 (which is missing in IFN-α2). Thus, papers using the "consensus" human IFN-α sequence numbering have all homologous positions above residue 43 one number higher than the specific sequence of HuIFN-α2 or its derivative IFN-α2/α1 (e.g., residue 120 in HuIFN-α2 is homologous to residue 121 in other human IFN-αs).

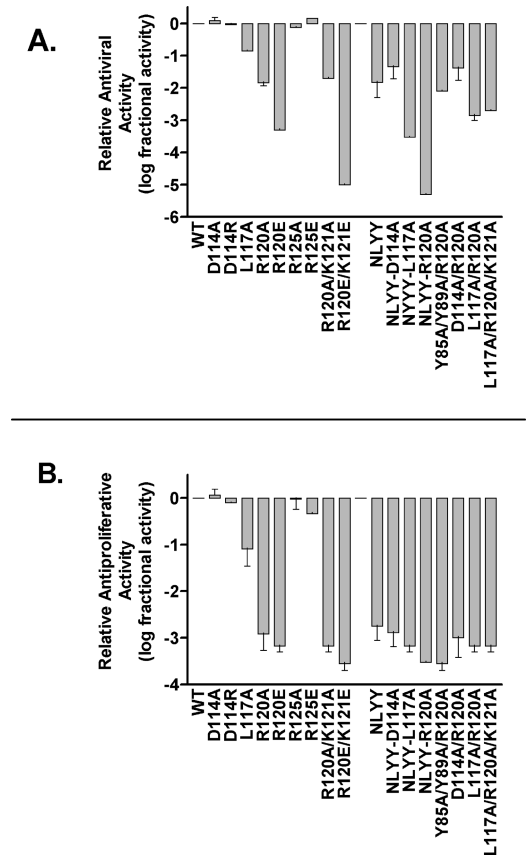

FIGURE 2: Antiviral and antiproliferative activity of human IFN-α2 mutants. For each mutant indicated, activity is presented as a fraction of the native IFN-α2, measured on human WISH cells. Thus, on the logarithmic scale, "0" is the baseline wild-type activity, and mutants show decreases of up to 5 logs of activity (this number represents no activity at the highest concentration of IFN mutant used in the assays; the mutants may have even less activity, as indicated by the designation of "≤" in Tables 1−3). Mutants were measured between one and five times each in independent assays. For multiple measurements, error bars indicate the standard error (SEM).

Table 1: Biological Activity and Binding to Human IFN Receptor Subunits of IFN-α2 and Its Mutants[a]

	antiviral activity (% of native EC_{50})			antiproliferative activity (% of native EC_{50})	binding affinity ratio $K_{D\,mut}/K_{D\,wt}$	
	human (WISH)	human (HeLa)	bovine (MDBK)	human (WISH)	IFNAR-1	IFNAR-2
IFN-α2	100	100	100	100	1	1
-114A	130	37	79	98	−	0.5
-117A	14	20	36	18	2.2	1.3
-120A	1.4	2.3	68	0.05	ND	1.4
-125A	76	90	100	83	−	0.8
-114R	86	49	94	46	−	0.4
-120E	≤0.05	<0.028	30	≤0.05	−	0.7
-120E-8CTail	−	<0.028	−	−	ND	0.14
-125E	113	167	−	41	−	0.9
-114A120A	1.7	1.0	11.7	0.2	−	1.2
-117A120A	0.15	<0.008	0.7	≤0.05	−	0.7
-120A121A	3.1	1.6	19	≤0.09	−	0.6
-120E121E	≤0.002	<1.3	10	≤0.02	−	0.8
-117A120A121A	0.3	≤0.016	4.9	≤0.05	7	1.1
-NLYY	1.3	1.8	39	≤0.1	ND	2.5
-NLYY-114A	1.9	1.0	13	0.05	−	0.9
-NLYY-117A	0.03	<0.03	13	≤0.05	−	1
-NLYY-120A	≤0.001	≤0.002	−	≤0.001	ND	−
-85A89A-120A	0.5	0.012	0.72	≤0.03	−	1.1

[a] The antiviral activity of IFN-α2 is (2−4) × 10^8 units/mg on human HeLa cells challenged with VSV, calibrated against an international standard for IFN-α2. The native sequence contains residues R120, K121, and R125. Binding affinity ratios are relative to wild-type IFN-α2 affinities toward IFNAR1 (K_D = 2 μM) and IFNAR2 (K_D = 2 nM). ND: not detected (binding below the detection limit of the measurement (K_D > 10 μM)). (−): not tested. NLYY = N65A/L80A/Y85A/Y89A.

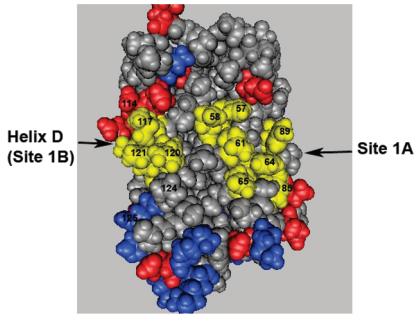

FIGURE 3: Residues interacting with IFNAR-1. Space-filling model showing residues of site 1A and important residues of helix D in yellow. Acidic residues are shown in red, basic in blue, and others in gray. Model generated using HuIFN-α2 coordinates (PDB 1ITF) with Cn3D (http://www.ncbi.nlm.nih.gov/Structure/CN3D/cn3d.shtml).

bovine MDBK cells that are generally highly sensitive to human IFN-αs and are often less sensitive to modification of HuIFN-α.

As expected, mutations in the D helix, including those such as R120E/K121E which decreased activity by more than 4 orders of magnitude, did not significantly change the binding affinity for human IFNAR-2 from that measured for native IFN-α2 ($K_D \approx 2.5 \pm 0.5$ nM), with almost all mutants being within 2-fold of this value (Table 1). Affinity of R120A for IFNAR-1 and of the 120E-8CTail mutant was decreased by at least 10-fold (ND: not detected), to the limits of detection of the experimental setup ($K_D \geq 10$ μM). Because of technical difficulties, we did not obtain reliable measurements of IFNAR-1 for some of the other samples. Nevertheless, the retention of high affinity for IFNAR-2 excludes direct interactions of helix D residues with human IFNAR-2. The locations of these functionally significant helix D residues and those on helices B and C (site 1A) are shown (Figure 3).

The Interaction of Site 1A and Helix D for IFN-α2 Activity and IFNAR-1 Binding. For the IFN-α2 variants, we investigated whether there is a functional relationship between previously identified residues ("site 1A") and the functionally important residues on helix D. We therefore combined alanine substitutions at each of the residues Asp114, Leu117, and Arg120 with the four-site alanine mutant in site 1A residues N65, L80, Y85, and Y89 ("NLYY") (Figure 2, Table 1). Although the NLYY mutant has about 1% activity on human HeLa cells, the R120A mutant combined with the NLYY mutants lacks measurable antiviral and antiproliferative activity. Also, the combination of L117A with NLYY significantly reduced activity on human cells from that of NLYY, although the L117A mutant itself only had small effects on biological activity. In contrast, the addition of the D114A mutation to NLYY seems to have little additional effect on the antiviral activity of NLYY on human cells. As with other site 1A and helix D mutants, these combined mutants retained affinity for IFNAR-2.

Helix D Residues Are Also Important for IFN-α2/α1 Activity and Binding to IFNAR-1. To examine residues involved in binding to IFNAR-1 in a different sequence context, we made homologous mutations in site 1A and in the D helix in the chimeric interferon IFN-α2/α1. This is a hybrid of human IFN-α2 (amino acids 1−61) and human IFN-α1 (residues 63−166). Most of the functionally important residues in the IFNAR-1 site are from the IFN-α1-derived segment of the chimera, rather than from the IFN-α2 N-terminal segment, although many residues are conserved between the two IFNs (Figure 1). This chimera is particularly interesting in that it has high biological activity on both human and murine cells, as well as those of other species (*42, 43*).

In IFN-α2/α1, alanine substitutions in site 1A residues (N65, L80, C85, Y89), including a three-site alanine substitution mutant (L80/C85/Y89) and a four-site alanine substitution mutant (N65/L80/C85/Y89), produced no more than a 2−3-fold decrease in antiviral activity on human and murine cells (Table 2). A five-site alanine substitution mutant that added Phe64Ala, located in the cluster with N64, C85, and Y89, produced a 10−20-fold decrease on the antiviral

Table 2: Antiviral and Antiproliferative Activities of IFN-α2/α1 and Its Site 1A Mutants[a]

	antiviral activity (% of native)				antiproliferative activity (% of native)	
	human (WISH)	human (HeLa)	murine (L-929)	bovine (MDBK)	human (WISH)	murine (NFS-01)
IFN-α2/α1	100	100	100	100	100	100
-85A	−	141	144	55	−	−
-89A	96	69	38	100	97	23
-80A[b]	19[b]	−	31	34	−	−
-85A89A	183	143	−	−	89	15
-80A85A89A	204	54	100	100	22	24
-65A80A85A89A	69	63	55	200	16	50
-65A80A85A89A-64A	11	4.2	−	−	2.1	0.38

[a] The antiviral activity of IFN-α2/α1 is $(1-2) \times 10^8$ units/mg on human HeLa cells challenged with VSV, calibrated against an international standard for IFN-α2. The native sequence of IFN-α2/α1 contains residues N65, L80, C85, and Y89. (−): not tested. [b] Assay on human A549 cells.

Table 3: Biological Activity and Binding to Human IFN Receptor Subunits of IFN-α2/α1 and Its Mutants[a]

	antiviral activity (% of native)				antiproliferative activity (% of native)		binding affinity ratio $K_{D\,mut}/K_{D\,wt\text{-}\alpha2}$	
	human (WISH)	human (HeLa)	murine (L-929)	bovine (MDBK)	human (WISH)	murine (NFS-01)	IFNAR-1	IFNAR-2
IFN-α2/α1	100	100	100	100	100	100	0.2	2.1
-120A	9.7	2	2	100	0.7	0.03	2.5	1.2
-120A/121A	13.8	8.3	33	100	0.5	8	4.5	1.3
-120E	≤0.02	<0.04	≤0.04	100	<0.02	≤0.0005	−	1.3
-120E/121E	0.006	<0.08	≤0.04	10	≤0.05	<0.0001	ND	1.5
-121E	−	8	0.5	100	−	−	1.7	1.2
-124E	−	20	100	100	−	−	1	1
-120E/121E/124E	<0.1	<0.04	<0.01	<0.08	<0.2	−	ND	6[b]

[a] The antiviral activity of IFN-α2/α1 is $(1-2) \times 10^8$ units/mg on human HeLa cells challenged with VSV, calibrated against an international standard for IFN-α2. The native sequence contains residues K120, K121, and R124. Binding affinity ratios are relative to wild-type IFN-α2 affinities toward IFNAR1 ($K_D = 2\ \mu M$) and IFNAR2 ($K_D = 2$ nM) and not relative to IFNα2/α1. (−): not tested. ND: not detected (binding below the detection limit of the measurement ($K_D > 10\ \mu M$)). [b] The dissociation rate (k_d) of this mutant from IFNAR2 is similar to wild-type IFN-α2. Change in the affinity stems from change in association rate (k_a), possibly due to the additional charges presented by the added negatively charged residues that act over long distances.

activity on human cells. A similar trend, but of larger magnitude, was obtained for the antiproliferative effects of IFN-α2/α1 mutants, measured on human WISH cells and murine NFS-01 cells. (The growth of HeLa cells and L-929 cells, used for the antiviral assays, was only weakly inhibited by native IFNs, so WISH cells and NFS-01 cells that responded more robustly to the antiproliferative effects of IFNs were used.) Thus, the site 1A cluster of residues of IFN-α2/α1 has less relative importance for binding to IFNAR-1 than this cluster has for IFN-α2.

Within this region, previous studies of a chimeric IFN-α21/α2c construct suggested that aspartic acid substitution of Cys86 (equivalent to Cys85 in IFN-α2/α1) strongly affected biological activity (*28*). However, substitution of Asp for Cys 85 in IFN-α2/α1, either as a single-site mutation or within the context of multisite mutants, did not markedly decrease antiviral activity on human or murine cells (data not shown). Thus, the effect of substitutions in site 1A of IFN-αs seems to depend strongly on the IFN-α subtype, i.e., the sequence context.

Contributions of positively charged D helix residues of IFN-α2/α1 were more dramatic (Table 3). In particular, the K120E mutation caused a loss of antiviral activity of >2500-fold on both human and murine cells. Relative antiproliferative activity was often at least 10-fold lower than antiviral activity (Table 3). Thus, residue 120 is important for both IFN-α2 and IFN-α2/α1 and for the interaction with both human and murine IFNAR-1. However, K120 mutants retained high antiviral activity on bovine MDBK cells, and high affinity for human IFNAR-2, demonstrating that the mutations do not affect global folding of the mutants. For interactions with the human and murine receptor, the positively charged residues have the relative importance K120 ≫ K121 > R124. Binding to human IFNAR-2, measured by SPR, was similar to the binding of native IFN-α2 and was not affected by these functionally significant mutations (Table 3). However, binding to human IFNAR-1-ECD was significantly weakened for mutants with lowered biological activity and was outside the measurement limit ($K_D > 10\ \mu M$) for mutants with little or no detectable activity on human cells. (It is also noteworthy that the affinity of IFN-α2/α1 for IFNAR-1 is about 5 times stronger than that of IFN-α2; i.e., the ratio of the K_D's of IFN-α2/α1 to that of IFN-α2 is about 0.2. This stronger binding of the native IFN-α2/α1 to IFNAR-1 makes changes in binding easier to measure, since the affinity is further from the upper limit of affinity of the experimental protocol.)

Mutants in Helix D and Site 1A That Lack Biological Activity Are Antagonists of in Vitro Biological Activity of IFN-α2. It is predicted that IFN variants with strong binding to IFNAR-2 and no significant binding to IFNAR-1 should act as competitive antagonists, as has been demonstrated for other cytokines that ligate two receptor subunits to initiate action (*44*−*46*). As predicted, mutants with no detectable antiviral and antiproliferative activity blocked a protective concentration of human IFN-α2 IFN activity in the antiviral assay (summarized in Table 4; Figure 4). These include the charge-reversal mutants R120E, R120E/K121E, and R120E-8CTail. In addition, although the four-site alanine substitution mutant NLYY, mutated on helices B and C, retains about 1% of its antiviral activity (i.e., it is a weak agonist), the combination of L117A or R120A with NLYY leads to the

Table 4: Antagonist Properties of Human IFN-α2 Variants

	antiviral activity[b]	antiproliferative activity[b]	antagonist activity[a]	
interferon form	human (WISH, %)	human (WISH, %)	antiviral IC_{50} (M)[c]	antiproliferative IC_{50} (M)[d]
IFN-α2 (wild type)	100	100	no	no
-114A	130	98	no	no
-117A	14	18	no	no
-120A	1.4	0.05	no	±
-120E	≤0.05	≤0.05	4.1×10^{-9}	5.3×10^{-9}
-125E	113	41	no	no
-117A120A	0.15	≤0.05	no	yes
-120A121A	3.1	≤0.09	no	±
-120E121E	≤0.002	≤0.02	2.1×10^{-9}	2.6×10^{-9}
-117A120A121A	0.3	≤0.05	±	yes
-NLYY[e]	1.3	≤0.1	no	no
-NLYY-117A	<0.03	≤0.05	4.1×10^{-8}	8.5×10^{-8}
-NLYY-120A	≤0.001	≤0.001	4.1×10^{-8}	1.7×10^{-7}
-85A89A-120A	0.5	≤0.03	−	yes

[a] "No" corresponds to agonist activity. (±): variable/weak. (−): not tested. "Yes": antagonism was demonstrated, but quantitative variability between assays does not permit direct comparison to the IC_{50} values reported for other mutants in this table. [b] Activity expressed as % of native EC_{50}. Antiviral assays of WISH cells challenged with VSV were as in refs *3* and *36*; antiproliferative assays were as in refs *13* and *50*. [c] Representative data, competing with 1.3×10^{-10} M IFN-α2 (HeLa cells). [d] Representative data, competing against 1.7×10^{-9} M IFN-α2 (WISH cells). [e] NLYY = N65A/L80A/Y85A/Y89A (*41*). The native sequence residues are D114, L117, R120, K121, and Q124.

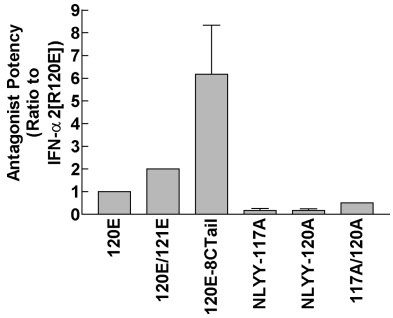

FIGURE 4: Comparison of antiviral antagonist potency for IFN-α2 mutants with antagonist activity. Relative potencies of antagonism of antiviral activity (measured on HeLa cells) are expressed as the ratio of IC_{50} values for different IFN-α2 mutants relative to that of IFN-α2[R120E]. Values derive from one to three independent measurements of each mutant, with an internal R120E mutant standard in each assay to correct for interassay variability of absolute IC_{50} values. Mutants with values higher than 1.0 have higher potency than IFN-α2[R120E], and values lower than 1.0 have lower potency than R120E.

loss of residual antiviral activity and the gain of antagonist function (Table 4).

The various mutants were also tested for their antagonism of antiproliferative activity (Table 4), with results parallel to those obtained in the antiviral assays. As expected from the antiviral results, the R120E, R120E/K121E, NLYY-117A, and NLYY-120A mutants are antagonists of IFN-α2. In addition, several mutants that preferentially lost antiproliferative activity while retaining low antiviral activity, such as R120A/K121A, L117A/R120A/K121A, and Y85A/Y89A/R120A, had weak antiproliferative antagonist activity.

The antagonists vary in their potencies (Figure 4, Table 4). The R120E/K121E and R120E mutants are more potent than the NLYY-117A and NLYY-120A mutants that require higher concentrations for antagonism. In addition, several mutants are only weakly inhibitory. We hypothesize that the greater potency derives from more complete disruption of the IFNAR-1 binding, although for all antagonists for which we have data, the binding to IFNAR-1 has a K_D of $\geq 10\ \mu M$. For the antiviral assays, the molar ratio of R120E to native IFN for full antagonism is 100−250. Since studies have demonstrated that cellular activation for some assays requires only 5−10% of receptor occupancy, it is likely that effective blockade of this activity requires almost complete saturation of receptors; in the antiviral assay, even a small number of unblocked receptors left unblocked by the antagonist for a short period would permit binding of native IFN and development of viral resistance. For antiproliferative assays, the molar ratio of R120E or R120E/K121E to native IFN for effective antagonism is lower (range 16−100), probably reflecting the need for sustained active IFN action for achieving antiproliferative effects.

An effective *in vivo* antagonist will require higher potency through stronger binding to IFNAR-2. As a first step, we constructed a derivative of the IFN-α2[R120E] mutant that also had substitutions in the C-terminal tail such that the C-terminus had the more basic sequence of IFN-α8 (KRLKSKE), rather than that of IFN-α2 (ESLRSKE), which we denote "120E-8CTail. It was previously shown that IFN-α8 binds more strongly to IFNAR-2 (*9, 21*) and that replacement of three amino acids in the C-terminus of native IFN-α2 by those found in IFN-α8 increases the affinity of the IFN-α2 C-terminal mutant for IFNAR-2 (*21*). Therefore, 120E-8CTail, with its higher affinity for IFNAR-2, was expected to have higher potency in the antagonism assay. This prediction was validated: 120E-8CTail can antagonize IFN-α2 at a concentration 4−8-fold lower than IFN-α2[R120E] (Figure 4).

DISCUSSION

Recent evidence implicating type I IFNs in the pathogenesis of systemic lupus erythematosus and possibly Sjögren's syndrome and other autoimmune diseases motivates the development of effective antagonists for type I IFNs (*6, 7*). The current strategy for a type I IFN antagonist is to disable the IFNAR-1 site while maintaining or improving the affinity of the IFNAR-2 site. An analogous strategy has been employed in developing ligand-based antagonists for other cytokines that require ligand-dependent ligation of two receptor subunits to initiate signaling (*44*−*46*). However, it was first necessary to more completely map the IFNAR-1 site and to find appropriate mutants in this site. The current

results document that appropriate mutants of the IFNAR-1 site can serve as competitive antagonists of *in vitro* activities of IFN-α2.

Most recent attempts to identify the IFNAR-1 site have focused on helices B and C and the connecting BC loop of IFN-α (*12, 27, 28, 41, 47*). The most complete mutagenesis study, which included affinity measurements with IFNAR-1 and IFNAR-2, demonstrated for IFN-α2 that Phe64, Tyr85, and Tyr89 of helices B and C form a patch that interacts directly with IFNAR-1 and plays a strong role in the biological activity in IFN-α2 (*41*). We refer to this region as "site 1A". However, while the four-point site 1A mutant ("NLYY") of IFN-α2 showed significant loss of activity, it was still a weak agonist, retaining 1% antiviral activity and 0.1% antiproliferative activity *in vitro* (*41*) (also Table 4).

The current data demonstrate that residues of the D helix are also part of the IFNAR-1 site and contribute to biological activity for two distinct IFN-αs, IFN-α2 and IFN-α2/α1 (Tables 1 and 3). Most dramatically, substitution of alanine at position 120 (Arg for IFN-α2; Lys for IFN-α2/α1) strongly decreases antiviral and antiproliferative activity on human cells and, for IFN-α2/α1, on murine cells. This is the first "hot-spot" residue reported for the interaction with IFNAR-1. Charge-reversal mutations at position 120 resulted in total or near-total loss of antiviral activity for both IFN-α2 and IFN-α2/α1. Significantly, the IFN-α2/α1[R120E] mutant lost activity on both human and murine cells (Table 3), demonstrating the conservation of sequence and function between the human and murine models. The importance of the conserved positive charge at position 120 suggests that it may form a salt bridge with a negative charge on human, murine, and possibly bovine IFNAR-1. In addition, Leu117, conserved in all human and murine type I IFNs, is also implicated in IFNAR-1 binding, particularly when L117A is combined with R120A. We would thus implicate the residues in order of importance R120 ≫ L117, with a lesser role for K/R121.

Our data on the contributions of the D helix follow several prior studies that demonstrated a role for the D helix in biological activity (*25*−*27, 31*−*33*). These findings varied widely in the IFNs used, the residues mutated, and the assays used, and most documented relatively small decreases in biological activity following mutagenesis. An exception is the study of Cheetham et al., where a two-site charge-reversal mutant of human IFN-α4 in the positions equivalent to R120 and K121 produced dramatic decreases of antiviral activity on human and bovine cells (*33*). Since that study preceded the determination of the three-dimensional structure of IFN or knowledge that the IFN receptor is heterodimeric, the authors could not provide a specific structural interpretation, as is now possible. It should be noted that at least one study with HuIFN-β also provided inferential data that residues of the D helix might interact with IFNAR-1 (*27*).

The relationship of the helix D residues to the previously identified site 1A is unknown, since we do not know the structure of the IFNAR-1/IFN complex. The simplest model would consider that the relevant residues on helix D are an extension of site 1A, forming an extended binding site on type I IFN for binding to a single binding site on IFNAR-1 (Figure 3). This view is consistent with the low-resolution structure of the IFN-α2/IFNAR-1-ECD/IFNAR-2-ECD complex as obtained by density modeling to a three-dimensional image reconstruction of negatively stained electron microscopy images (Figure 5) (*23*). Indeed, in this model, R120 is perfectly located to interact with IFNAR-1 and is proximal to an aspartic acid on IFNAR-1, making this salt bridge a testable hypothesis. A possible, but less likely, alternative is that the residues on helix D may be part of a site proximal to site 1A, but distinct from it, so that R120 interacts with a second site on IFNAR-1, physically separate from the site binding to site 1A. Multisite interactions between IFNAR-1 and IFNs could also be consistent with the low-resolution model of the ternary IFN/IFNAR-1/IFNAR-2 complex derived from electron microscopy (*23*) and might provide greater opportunities for discriminating among the type I IFNs and modulating cellular responses. This scenario is reminiscent of the IL-1 receptor (IL-1R) binding interaction where the three extracellular immunoglobulin-like domains of IL-1R wrap around the IL-1β and IL-1RA ligands (*48, 49*). However, for the IFN/IFNAR-1 interaction, we await more structural data.

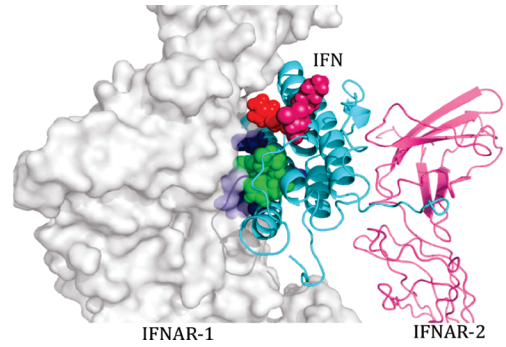

FIGURE 5: Representation of the IFN/IFNAR-1/IFNAR-2 complex as revealed by mutagenesis on the ternary structure derived from electron microscopy and modeling (*23*). For the IFNAR-1 site, in blue are IFN residues 64, 65, 80, 85, and 89 (site 1A). In green are residues 57, 58, and 61. In magenta are residues D114 and L117, and in red is the "hot-spot" residue, R120.

We have also demonstrated that mutants of HuIFN-α2 with deficient binding to IFNAR-1, and no detectable antiviral or antiproliferative activity, can function as novel antagonists of native IFN-α2 in antiviral and antiproliferative assays.[2] The results fit a simple biophysical model of binding to a heterodimeric receptor, where decreasing or eliminating binding to one receptor subunit, while maintaining or enhancing binding to the other receptor subunit, can be used to generate and optimize antagonist activity. The antiviral assay, in particular, is a stringent test of antagonism, since small amounts of native IFN, acting during a short incubation, are sufficient to trigger antiviral protection. Thus, any

[2] An early report of an IFN with antagonist properties, the human triple mutant, IFN-α2[L30A/D32A/R33A] (*1*), is instructive but quite different from the current antagonists. This mutant lacked biological activity on both human WISH and bovine MDBK cells but acted as a binding antagonist only on bovine cells, not on human cells. Knowing now that this mutation is in the IFNAR-2 binding site, a likely explanation is clear: for human cells, the mutation weakened the high-affinity binding to IFNAR-2, and the mutant was simply inactive; it could only bind weakly to IFNAR-1, which was insufficient to compete with other IFNs. However, even though effective binding to bovine IFNAR-2 may have also been disrupted, as demonstrated by loss of biological activity, the serendipitously high affinity of HuIFN-α2 for bovine IFNAR-1 (*2, 3*) permitted the mutant to block binding of native HuIFN-α2 to the cells through its high-affinity binding to bovine IFNAR-1.

antagonist must be present at sufficient concentration and have sufficient affinity for IFNAR-2 to effectively block the receptor. These IFN antagonists also provide further pharmacological evidence that recruitment of IFNAR-1 is required for the activities measured.

These novel antagonists are useful for *in vitro* inhibition of IFN. The current limitation for *in vivo* or therapeutic use is their potency, which reflects their affinity for IFNAR-2. Derived from IFN-α2, the antagonists have a K_D for IFNAR-2 of 1−3 nM, requiring them to be in high molar excess of native IFNs, some of which have even higher affinity for IFNAR-2 than does IFN-α2 (*9*). As a first step toward increasing potency, we demonstrated that changes in the C-terminus of the IFN-α2[R120E] mutant to produce the 120E-8CTail mutant increased the potency of antagonism, as expected from its higher affinity for IFNAR-2 (Table 1, Figure 4) (*21*).

Several of the mutated residues, such as the positively charged position 120, are conserved in IFNs from other species, and we demonstrated that the IFN-α2/α1[R120E] mutant lacked antiviral and antiproliferative activity on *both* human and murine cells (Table 3). Thus, mutation of equivalent residues may provide competitive antagonists for these species.

The data reported here add to our understanding of the IFNAR-1 binding site on type I IFNs and form the basis for developing novel antagonistic type I IFN analogues that may provide useful alternatives to the more common antibody-based and receptor-based antagonists. Building on the examples reported here, it should be possible to develop antagonists with higher affinity for IFNAR-2 that will have the potency required for *in vivo* and therapeutic use.

ACKNOWLEDGMENT

We thank Dr. Lara Izotova (UMDNJ—Robert Wood Johnson Medical School) and Dr. Sergei Kotenko (UMDNJ—New Jersey Medical School) for helpful discussions.

REFERENCES

1. Marcucci, F., and De Maeyer, E. (1986) An interferon analogue, [Ala 30,32,33]HuIFN-alpha 2, acting as a HuIFN-alpha 2 antagonist on bovine cells. *Biochem. Biophys. Res. Commun. 134*, 1412–1418.
2. Mouchel-Vielh, E., Lutfalla, G., Mogensen, K. E., and Uze, G. (1992) Specific antiviral activities of the human alpha interferons are determined at the level of receptor (IFNAR) structure. *FEBS Lett. 313*, 255–259.
3. Lim, J. K., and Langer, J. A. (1993) Generation and characterization of anti-idiotypic antibodies recognizing the interferon-alpha receptor: implications for ligand-receptor interactions. *J. Interferon Res. 13*, 295–301.
4. Langer, J. A. (2007) *Type I Interferons: Something Old, Something New, in Class II Cytokines* (Zdanov, A., Ed.) pp 15−49, Transworld Research Network, Kerala, India.
5. Pestka, S., Krause, C. D., and Walter, M. R. (2004) Interferons, interferon-like cytokines, and their receptors. *Immunol. Rev. 202*, 8–32.
6. Crow, M. K. (2005) Interferon pathway activation in systemic lupus erythematosus. *Curr. Rheumatol. Rep. 7*, 463–468.
7. Pascual, V., Farkas, L., and Banchereau, J. (2006) Systemic lupus erythematosus: all roads lead to type I interferons. *Curr. Opin. Immunol. 18*, 676–682.
8. Cutrone, E. C., and Langer, J. A. (1997) Contributions of cloned type I interferon receptor subunits to differential ligand binding. *FEBS Lett. 404*, 197–202.
9. Jaks, E., Gavutis, M., Uze, G., Martal, J., and Piehler, J. (2007) Differential receptor subunit affinities of type I interferons govern differential signal activation. *J. Mol. Biol. 366*, 525–539.
10. Uze, G., Schreiber, G., Piehler, J., and Pellegrini, S. (2007) The receptor of the type I interferon family. *Curr. Top. Microbiol. Immunol. 316*, 71–95.
11. Cutrone, E. C., and Langer, J. A. (2001) Identification of critical residues in bovine IFNAR-1 responsible for interferon binding. *J. Biol. Chem. 276*, 17140–17148.
12. Cajean-Feroldi, C., Nosal, F., Nardeux, P. C., Gallet, X., Guymarho, J., Baychelier, F., Sempe, P., Tovey, M. G., Escary, J. L., and Eid, P. (2004) Identification of residues of the IFNAR1 chain of the type I human interferon receptor critical for ligand binding and biological activity. *Biochemistry 43*, 12498–12512.
13. Jaitin, D. A., Roisman, L. C., Jaks, E., Gavutis, M., Piehler, J., Van der, H. J., Uze, G., and Schreiber, G. (2006) Inquiring into the differential action of interferons (IFNs): an IFN-alpha2 mutant with enhanced affinity to IFNAR1 is functionally similar to IFN-beta. *Mol. Cell. Biol. 26*, 1897.
14. Gavutis, M., Lata, S., Lamken, P., Muller, P., and Piehler, J. (2005) Lateral ligand-receptor interactions on membranes probed by simultaneous fluorescence-interference detection. *Biophys. J. 88*, 4289–4302.
15. Lamken, P., Lata, S., Gavutis, M., and Piehler, J. (2004) Ligand-induced assembling of the type I interferon receptor on supported lipid bilayers. *J. Mol. Biol. 341*, 303–318.
16. Piehler, J., and Schreiber, G. (1999) Mutational and structural analysis of the binding interface between type I interferons and their receptor Ifnar2. *J. Mol. Biol. 294*, 223–237.
17. Chill, J. H., Quadt, S. R., Levy, R., Schreiber, G., and Anglister, J. (2003) The human type I interferon receptor: NMR structure reveals the molecular basis of ligand binding. *Structure 11*, 791–802.
18. Roisman, L. C., Piehler, J., Trosset, J. Y., Scheraga, H. A., and Schreiber, G. (2001) Structure of the interferon-receptor complex determined by distance constraints from double-mutant cycles and flexible docking. *Proc. Natl. Acad. Sci. U S.A. 98*, 13231–13236.
19. Quadt-Akabayov, S. R., Chill, J. H., Levy, R., Kessler, N., and Anglister, J. (2006) Determination of the human type I interferon receptor binding site on human interferon-alpha2 by cross saturation and an NMR-based model of the complex. *Protein Sci. 15*, 2656–2668.
20. Piehler, J., Roisman, L. C., and Schreiber, G. (2000) New structural and functional aspects of the type I interferon-receptor interaction revealed by comprehensive mutational analysis of the binding interface. *J. Biol. Chem. 275*, 40425–40433.
21. Slutzki, M., Jaitin, D. A., Yehezkel, T. B., and Schreiber, G. (2006) Variations in the unstructured C-terminal tail of interferons contribute to differential receptor binding and biological activity. *J. Mol. Biol. 360*, 1019–1030.
22. Lamken, P., Gavutis, M., Peters, I., Van der, H. J., Uze, G., and Piehler, J. (2005) Functional cartography of the ectodomain of the type I interferon receptor subunit ifnar1. *J. Mol. Biol. 350*, 476–488.
23. Li, Z., Strunk, J. J., Lamken, P., Piehler, J., and Walz, T. (2008) The EM structure of a Type I Interferon-receptor complex reveals a novel mechanism for cytokine signaling. *J. Mol. Biol. 377*, 715–724.
24. Strunk, J. J., Gregor, I., Becker, Y., Li, Z., Gavutis, M., Jaks, E., Lamken, P., Walz, T., Enderlein, J., and Piehler, J. (2008) Ligand binding induces a conformational change in ifnar1 that is propagated to its membrane-proximal domain. *J. Mol. Biol. 377*, 725–739.
25. Mitsui, Y., Senda, T., Shimazu, T., Matsuda, S., and Utsumi, J. (1993) Structural, functional and evolutionary implications of the three-dimensional crystal structure of murine interferon-β. *Pharmacol. Ther. 58*, 93–132.
26. Runkel, L., Pfeffer, L., Lewerenz, M., Monneron, D., Yang, C. H., Murti, A., Pellegrini, S., Goelz, S., Uze, G., and Mogensen, K. (1998) Differences in activity between alpha and beta type I interferons explored by mutational analysis. *J. Biol. Chem. 273*, 8003–8008.
27. Runkel, L., DeDios, C., Karpusas, M., Betzenhauser, M., Muldowney, C., Zafari, M., Benjamin, C. D., Miller, S., Hochman, P. S., and Whitty, A. (2000) Systematic mutational mapping of sites on human interferon-beta-1a that are important for receptor binding and functional activity. *Biochemistry 39*, 2538–2551.
28. Hu, R., Bekisz, J., Schmeisser, H., McPhie, P., and Zoon, K. (2001) Human IFN-alpha protein engineering: the amino acid residues at positions 86 and 90 are important for antiproliferative activity. *J. Immunol. 167*, 1482–1489.

29. Kalie, E., Jaitin, D. A., Abramovich, R., and Schreiber, G. (2007) An interferon alpha2 mutant optimized by phage display for IFNAR1 binding confers specifically enhanced antitumor activities. *J. Biol. Chem. 282*, 11602–11611.
30. Langer, J. A. (2007) Interferon at 50: new molecules, new potential, new (and old) questions. *Sci. STKE 2007*, e53.
31. Weber, H., Valenzuela, D., Lujber, G., Gubler, M., and Weissmann, C. (1987) Single amino acid changes that render human IFN-alpha 2 biologically active on mouse cells. *EMBO J. 6*, 591–598.
32. Tymms, M. J., McInnes, B., Waine, G. J., Cheetham, B. F., and Linnane, A. W. (1989) Functional significance of amino acid residues within conserved hydrophilic regions in human interferons-alpha. *Antiviral Res. 12*, 37–47.
33. Cheetham, B. F., McInnes, B., Mantamadiotis, T., Murray, P. J., Alin, P., Bourke, P., Linnane, A. W., and Tymms, M. J. (1991) Structure-function studies of human interferons-alpha: enhanced activity on human and murine cells. *Antiviral Res. 15*, 27–39.
34. Valente, C. A., Prazeres, D. M., Cabral, J. M., and Monteiro, G. A. (2004) Translational features of human alpha 2b interferon production in Escherichia coli. *Appl. Environ. Microbiol. 70*, 5033–5036.
35. Arakawa, T., and Tsumoto, K. (2003) The effects of arginine on refolding of aggregated proteins: not facilitate refolding, but suppress aggregation. *Biochem. Biophys. Res. Commun. 304*, 148–152.
36. Familletti, P. C., Rubinstein, S., and Pestka, S. (1981) A convenient and rapid cytopathic effect inhibition assay for interferon. *Methods Enzymol. 78*, 387–394.
37. Langer, J. A., Yang, J., Carmillo, P., and Ling, L. E. (1998) Bovine type I interferon receptor protein BoIFNAR-1 has high-affinity and broad specificity for human type I interferons. *FEBS Lett. 421*, 131–135.
38. Goldman, L. A., Zafari, M., Cutrone, E. C., Dang, A., Brickelmeier, M., Runkel, L., Benjamin, C. D., Ling, L. E., and Langer, J. A. (1999) Characterization of antihuman IFNAR-1 monoclonal antibodies: epitope localization and functional analysis. *J. Interferon Cytokine Res. 19*, 15–26.
39. Novick, D., Nabioullin, R. R., Ragsdale, W., McKenna, S., Weiser, W., Garone, L., Burkins, C., Kim, S. H., Rubinstein, M., Tepper, M. A., and Arulanandam, A. R. (2000) The neutralization of type I IFN biologic actions by anti-IFNAR-2 monoclonal antibodies is not entirely due to inhibition of Jak-Stat tyrosine phosphorylation. *J. Interferon Cytokine Res. 20*, 971–982.
40. Piehler, J., and Schreiber, G. (2001) Fast transient cytokine-receptor interactions monitored in real time by reflectometric interference spectroscopy. *Anal. Biochem. 289*, 173–186.
41. Roisman, L. C., Jaitin, D. A., Baker, D. P., and Schreiber, G. (2005) Mutational analysis of the IFNAR1 binding site on IFNalpha2 reveals the architecture of a weak ligand-receptor binding-site. *J. Mol. Biol. 353*, 271–281.
42. Weck, P. K., Apperson, S., Stebbing, N., Gray, P. W., Leung, D., Shepard, H. M., and Goeddel, D. V. (1981) Antiviral activities of hybrids of two major human leukocyte interferons. *Nucleic Acids Res. 9*, 6153–6166.
43. Rehberg, E., Kelder, B., Hoal, E. G., and Pestka, S. (1982) Specific molecular activities of recombinant and hybrid leukocyte interferon. *J. Biol. Chem. 257*, 11497–11502.
44. Mann, A., Niekisch, K., Schirmacher, P., and Blessing, M. (2006) Granulocyte-macrophage colony-stimulating factor is essential for normal wound healing. *J. Invest. Dermatol. Symp. Proc. 11*, 87–92.
45. van der Lely, A. J., and Kopchick, J. J. (2006) Growth hormone receptor antagonists. *Neuroendocrinology 83*, 264–268.
46. Jazayeri, J. A., De Weerd, N., Raye, W., Kivivuori, S., Zabihi, E., and Carroll, G. J. (2007) In vitro evaluation of leukemia inhibitory factor receptor antagonists as candidate therapeutics for inflammatory arthritis. *J. Interferon Cytokine Res. 27*, 281–289.
47. Di Marco, S., Grutter, M. G., Priestle, J. P., and Horisberger, M. A. (1994) Mutational analysis of the structure-function relationship in interferon-alpha. *Biochem. Biophys. Res. Commun. 202*, 1445–1451.
48. Vigers, G. P., Anderson, L. J., Caffes, P., and Brandhuber, B. J. (1997) Crystal structure of the type-I interleukin-1 receptor complexed with interleukin-1beta. *Nature 386*, 190–194.
49. Schreuder, H., Tardif, C., Trump-Kallmeyer, S., Soffientini, A., Sarubbi, E., Akeson, A., Bowlin, T., Yanofsky, S., and Barrett, R. W. (1997) A new cytokine-receptor binding mode revealed by the crystal structure of the IL-1 receptor with an antagonist. *Nature 386*, 194–200.
50. Evinger, M., Rubinstein, M., and Pestka, S. (1981) Antiproliferative and antiviral activities of human leukocyte interferons. *Arch. Biochem. Biophys. 210*, 319–329.

BI801588G